Available online at www.sciencedirect.com
SCIENCE DIRECT®
Journal of Sound and Vibration 292 (2006) 710–725
JOURNAL OF SOUND AND VIBRATION
www.elsevier.com/locate/jsvi

Harmonic response of adjacent structures connected with a friction damper

A.V. Bhaskararao, R.S. Jangid*

Department of Civil Engineering, Indian Institute of Technology Bombay, Powai, Mumbai 400 076, India

Received 6 April 2005; received in revised form 24 August 2005; accepted 26 August 2005
Available online 5 December 2005

Abstract

The dynamic behavior of two adjacent single-degree-of-freedom structures connected with a friction damper is investigated under harmonic ground acceleration. The governing differential equations of motion of the coupled system are derived and solved for analytical harmonic response during the non-slip and slip motion in friction damper. The response of the coupled system under harmonic excitation is found to be periodic occurring in three different modes of vibration (i.e. stick–stick, stick–slip and slip–slip modes). The closed-form expressions in terms of system parameters and excitation were derived for necessary conditions to initiate the stick–stick and slip–slip modes. A parametric study is also conducted to study the influence of important system parameters on the response behavior of damper connected structures. The important parameters included are structure damping ratios, frequency ratio, mass ratio and damper slip force. It was observed that there exists an optimum slip force in the damper for which the peak displacement of a structure attains the minimum value. The friction damper with optimum slip force significantly reduces the dynamic response of the coupled structures. Finally, the influence of important parameters on the maximum displacement of friction damper is also investigated for its effective design in coupling the adjacent structures.

1. Introduction

Structural vibration control, as an advanced technology in engineering, consists of implementing energy dissipation devices or control systems into structures to reduce excessive structural vibration, enhance human comfort and prevent catastrophic structural failure due to strong winds and earthquakes, among other inputs. Structural control technology can also be used for retrofitting of the historical structures, especially against earthquakes. The common sense approach to vibration control of structures consists of adding damping, either passively or actively. The damping dissipates some of the vibration energy of a structure by either transforming it to heat or transferring it directly to any connected structure or mass damper. The most common ways of adding damping to structures are by utilizing viscoelastic material as well as dashpots, and appending the structures with control devices. Effective damping can result by properly treating the structure, which is not damped adequately with viscoelastic materials. In addition, viscous dampers, tuned mass dampers (dynamic absorbers), friction dampers, shunted piezoceramics dampers, and magnetic dampers are other mechanisms that are used for passive vibration control [1].

*Corresponding author. Tel.: +91 22 2572 2545; fax: +91 22 2572 3480.
E-mail address: rsjangid@civil.iitb.ac.in (R.S. Jangid).

0022-460X/$ - see front matter © 2005 Elsevier Ltd. All rights reserved.
doi:10.1016/j.jsv.2005.08.029

Among the various control techniques, the coupling of two adjacent structures with suitable mechanisms can be preferred over the others (when possible). The main reason is that the installation of such devices does not require additional space and the free space available between two adjacent structures can be effectively utilized for placing the control devices. Such types of arrangement are also helpful in reducing the mutual pounding of structures occurred in the past major seismic events such as 1985 Mexico City and 1989 Loma Prieta earthquakes. Westermo [2] investigated the effectiveness of hinged links for connecting two neighboring floors of buildings to prevent mutual pounding.

The hinged link alters the dynamic characteristics of the connected structures and reduces the chances of pounding phenomenon. Luco and Barros [3] investigated the optimal values for the distribution of viscous dampers interconnecting two adjacent structures of different heights. It was observed that under certain conditions apparent high damping ratios could be achieved by the dampers in various modes of lightly damped structures. Zhang and Xu [4] studied the effectiveness of fluid dampers connecting multistory buildings under earthquake excitation. Zhu and Iemura [5] examined the dynamic characteristics of two single-degree-freedom systems coupled with a viscoelastic damper under stationary white-noise base excitation. Ni et al. [6] developed a method for analyzing the random seismic response of a structural system consisting of two adjacent buildings interconnected by nonlinear hysteretic damping devices. Although, the above studies confirm the effectiveness of different passive dampers in reducing the seismic response of connected structures, however, it will be interesting to study the dynamic behavior of two adjacent structures connected with friction dampers. The friction dampers were found to be very effective for earthquake resistant design of structures as well as retrofit of existing constructions [7–10].

In this paper, the dynamic response of two adjacent single story building structures connected with a friction damper is investigated under harmonic ground excitation. The specific objectives of the study are: (i) to derive the closed-form solutions for the harmonic response of the coupled system during stick and slip phases in the friction damper; (ii) to investigate the existence and necessary conditions for three different types of motion of the coupled system, such as stick–stick, stick–slip and slip–slip; (iii) to ascertain the existence of an optimum slip force in the friction damper for minimum displacement response of the coupled structures; and (iv) to examine the effects of important parameters such as damping ratio, mass ratio and slip force on the performance of the damper (for its effective design).

2. Harmonic response of damper connected system

Consider the two adjacent structures connected with friction damper as shown in Fig. 1(a). The friction damper provides a practical, economical and effective approach for the design of structures to resist excessive vibrations. The friction damper has advantages such as simple mechanism, low cost, less maintenance and powerful energy dissipation capability as compared to other passive dampers. The adjacent structures are idealized as single-degree-of-freedom systems and referred as Structure-1 and -2. The frictional force mobilized in the damper has typical Coulomb-friction characteristics. The corresponding mechanical model of the structures connected with friction damper is shown in Fig. 1(b). Let m_1, c_1 and k_1 be the mass, damping coefficient and stiffness, respectively of the Structure-1. The natural frequency and damping ratio of the Structure-1 are $\omega_1 = \sqrt{k_1/m_1}$ and $\xi_1 = c_1/2\sqrt{k_1 m_1}$, respectively. The m_2, c_2, k_2, $\omega_2 = \sqrt{k_2/m_2}$ and $\xi_2 = c_2/2\sqrt{k_2 m_2}$ denote the corresponding parameters of Structure-2. The system is subjected to harmonic ground motion. Depending upon the system parameters and excitation level, the connected structures may vibrate together without any slip in the friction damper (referred as non-slip mode) or vibrate independently if frictional force in the damper exceeds the limiting value (i.e. vibration in the slip mode).

2.1. Non-slip mode

During the non-slip mode, both structures vibrate together as a single-degree-of-system under ground excitation. The governing equation of motion of the combined system is expressed by

$$m_c\ddot{x}_c + c_c\dot{x}_c + k_c x_c = -m_c a_0 \sin(\omega t), \tag{1}$$

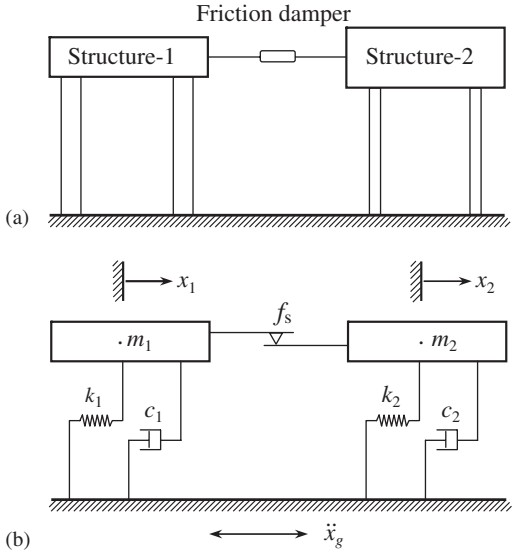

Fig. 1. Adjacent structures connected with a friction damper and its mechanical model: (a) adjacent structures with friction damper; (b) mechanical model.

where $m_c = m_1 + m_2$, $c_c = c_1 + c_2$ and $k_c = k_1 + k_2$ are the mass, damping coefficient and stiffness of the combined system, respectively; x_c, $\dot{x}_c$ and $\ddot{x}_c$ are the displacement, velocity and acceleration of the combined system, respectively; and a_0 and ω are the amplitude and frequency of the ground acceleration, respectively.

Let $x_c(t_0)$ and $\dot{x}_c(t_0)$ denote the displacement and the velocity, respectively, at $t = t_0$, then the general solution of Eq. (1) is expressed by[13]

$$\begin{bmatrix} x_c(t) \\ \dot{x}_c(t) \end{bmatrix} = A_{\mathrm{st}}(t - t_0) \begin{bmatrix} x_c(t_0) \\ \dot{x}_c(t_0) \end{bmatrix} + B_{\mathrm{st}}(t - t_0), \tag{2}$$

$$A_{\mathrm{st}}(\tau) = \mathrm{e}^{-\xi_c \omega_c \tau} \begin{bmatrix} \dfrac{\xi_c}{\sqrt{1-\xi_c^2}} \sin \omega_c' \tau + \cos \omega_c' \tau & \dfrac{1}{\omega_c'} \sin \omega_c' \tau \\ -\dfrac{\omega_c}{\sqrt{1-\xi_c^2}} \sin \omega_c' \tau & -\dfrac{\xi_c}{\sqrt{1-\xi_c^2}} \sin \omega_c' \tau + \cos \omega_c' \tau \end{bmatrix}, \tag{3}$$

$$B_{\mathrm{st}}(\tau) = \frac{a_0}{\omega_c^2} \begin{bmatrix} \mathrm{e}^{-\xi_c \omega_c \tau} \left\{ -b \left[\frac{\xi_c}{\sqrt{1-\xi_c^2}} \sin \omega_c' \tau + \cos \omega_c' \tau \right] - \frac{a\omega}{\omega_c'} \sin \omega_c' \tau \right\} \\ \quad + a \sin \omega t + b \cos \omega t \\ \mathrm{e}^{-\xi_c \omega_c \tau} \left\{ \frac{b\omega_c}{\sqrt{1-\xi_c^2}} \sin \omega_c' \tau + a\omega \left[\frac{\xi_c}{\sqrt{1-\xi_c^2}} \sin \omega_c' \tau - \cos \omega_c' \tau \right] \right\} \\ \quad + a\omega \cos \omega t - b\omega \sin \omega t \end{bmatrix}, \tag{4}$$

$$a = \frac{\left(1 - \frac{\omega^2}{\omega_c^2}\right) \cos \omega t_0 + 2\xi_c \frac{\omega}{\omega_c} \sin \omega t_0}{\left(1 - \frac{\omega^2}{\omega_c^2}\right)^2 + \left(2\xi_c \frac{\omega}{\omega_c}\right)^2}, \tag{5}$$

$$b = \frac{\left(1 - \frac{\omega^2}{\omega_c^2}\right) \sin \omega t_0 - 2\xi_c \frac{\omega}{\omega_c} \cos \omega t_0}{\left(1 - \frac{\omega^2}{\omega_c^2}\right)^2 + \left(2\xi_c \frac{\omega}{\omega_c}\right)^2}, \tag{6}$$

where $\omega_c = \sqrt{k_c/m_c}$, $\xi_c = c_c/2\sqrt{k_c m_c}$ and $\omega_c' = \omega_c\sqrt{1-\xi_c^2}$ denote the natural frequency, damping ratio and damped natural frequency of the combined system, respectively.

It is to be noted that the first term in the right-hand side of Eq. (2) accounts only for the transient response while the second term includes both the steady-state response and the remaining part of the transient one. It can be easily verified that $A_{st}(0) = I$ and $B_{st}(0) = \{1 \cdot 1\}^T$ for any a and b (where I denotes an identity matrix of size 2×2).

The coupled system remains in the non-slip mode until the frictional force in the damper is less than the limiting frictional force. The frictional force in the damper can be obtained by considering the dynamic equilibrium of Structure-1 or -2. Thus, the non-slip mode of the damper is valid until the following inequalities hold good

$$|m_1\ddot{x}_c + m_1 a_0 \sin(\omega t) + c_1\dot{x}_c + k_1 x_c| \leqslant f_s \tag{7a}$$

or

$$|m_2\ddot{x}_c + m_2 a_0 \sin(\omega t) + c_2\dot{x}_c + k_2 x_c| \leqslant f_s, \tag{7b}$$

where f_s is the limiting force in the friction damper and it is referred as slip force.

2.2. Slip mode

Whenever the force in friction damper attains to the slip force, the system moves into the slip mode. The condition for initiation of slippage is written as

$$\left|m_1\ddot{x}_1(t) + m_1 a_0 \sin(\omega t) + c_1\dot{x}_1(t) + k_1 x_1(t)\right| > f_s \tag{8a}$$

or

$$|m_2\ddot{x}_2(t) + m_2 a_0 \sin(\omega t) + c_2\dot{x}_2(t) + k_2 x_2(t)| > f_s, \tag{8b}$$

where x_1 and x_2 are the displacements relative to the ground of Structure-1 and -2, respectively.

The equations of motion of two connected structures in the slip mode are expressed by

$$m_1\ddot{x}_1 + c_1\dot{x}_1 + k_1 x_1 = -m_1 a_0 \sin(\omega t) + f_s \operatorname{sgn}(\dot{x}_2 - \dot{x}_1), \tag{9}$$

$$m_2\ddot{x}_2 + c_2\dot{x}_2 + k_2 x_2 = -m_2 a_0 \sin(\omega t) - f_s \operatorname{sgn}(\dot{x}_2 - \dot{x}_1), \tag{10}$$

where sgn denotes the signum function.

Let $x_1(t_0^*)$ and $\dot{x}_1(t_0^*)$ denote the displacement and the velocity, respectively, of the Structure-1 at time, $t = t_0^*$, then the general solution of Eq. (9) is given by

$$\begin{bmatrix} x_1(t) \\ \dot{x}_1(t) \end{bmatrix} = A_{sl}(t - t_0^*)\begin{bmatrix} x_1(t_0^*) \\ \dot{x}_1(t_0^*) \end{bmatrix} + B_{sl}(t - t_0^*), \tag{11}$$

$$A_{sl}(\tau^*) = e^{-\xi_1\omega_1\tau^*}\begin{bmatrix} \dfrac{\xi_1}{\sqrt{1-\xi_1^2}}\sin\omega_1'\tau^* + \cos\omega_1'\tau^* & \dfrac{1}{\omega_1'}\sin\omega_1'\tau^* \\ -\dfrac{\omega_1}{\sqrt{1-\xi_1^2}}\sin\omega_1'\tau^* & -\dfrac{\xi_1}{\sqrt{1-\xi_1^2}}\sin\omega_1'\tau^* + \cos\omega_1'\tau^* \end{bmatrix}, \tag{12}$$

$$B_{sl}(\tau^*) = \frac{a_0}{\omega_1^2}\begin{bmatrix} e^{-\xi_1\omega_1\tau^*}\left\{-(b'+d)\left[\dfrac{\xi_1}{\sqrt{1-\xi_1^2}}\sin\omega_1'\tau^* + \cos\omega_1'\tau^*\right] - \dfrac{a'\omega}{\omega_1'}\sin\omega_1'\tau^*\right\} \\ +a'\sin\omega\tau^* + b'\cos\omega\tau^* + d \\ e^{-\xi_1\omega_1\tau^*}\left\{\dfrac{\omega_1}{\sqrt{1-\xi_1^2}}\sin\omega_1'\tau^*(b'+d) + a'\omega\left[\dfrac{\xi_1}{\sqrt{1-\xi_1^2}}\sin\omega_1'\tau^* - \cos\omega_1'\tau^*\right]\right\} \\ +a'\omega\cos\omega\tau^* - b'\omega\sin\omega\tau^* \end{bmatrix}, \tag{13}$$

$$a' = \frac{\left(1-\frac{\omega^2}{\omega_1^2}\right)\cos\omega t_0^* + 2\xi_1\frac{\omega}{\omega_1}\sin\omega t_0^*}{\left(1-\frac{\omega^2}{\omega_1^2}\right)^2 + \left(2\xi_1\frac{\omega}{\omega_1}\right)^2}, \tag{14}$$

$$b' = \frac{\left(1-\frac{\omega^2}{\omega_1^2}\right)\sin\omega t_0^* - 2\xi_1\frac{\omega}{\omega_1}\cos\omega t_0^*}{\left(1-\frac{\omega^2}{\omega_1^2}\right)^2 + \left(2\xi_1\frac{\omega}{\omega_1}\right)^2}, \tag{15}$$

$$d = \frac{f_s}{m_1}\operatorname{sgn}(\dot{x}_2 - \dot{x}_1), \tag{16}$$

where $\omega_1' = \omega_1\sqrt{1-\xi_1^2}$ is the damped natural frequency of Structure-1.

The corresponding dynamic responses of Structure-2 during slip mode can be obtained using Eqs. (11)–(16) by interchanging the subscripts 1 and 2.

The coupled system remains in the slip mode till the relative velocity in the friction damper becomes zero i.e. $\dot{x}_1(t) = \dot{x}_2(t)$. At this point of time, there are two possibilities depending upon the system parameters and excitation level namely: (i) the reattachment of the two structures which is referred as stick–slip mode and (ii) occurrence of another slip mode in which the damper starts slipping in the opposite direction immediately and this is referred as slip–slip mode.

3. Conditions for three periodic motions

Depending upon the properties of the coupled system and excitation, the resulting harmonic response of the system is found to be periodic consisting of three different modes i.e. stick–stick, stick–slip and slip–slip mode. Such phenomenon had been observed in the past for various systems with sliding interface under harmonic ground excitation [11–14]. In order to ascertain this behavior of the present system, time variation of velocities of two structures (i.e. $\dot{x}_1(t)$ and $\dot{x}_2(t)$) is plotted in Fig. 2 for three different values of damper slip force (i.e. $f_s/a_0m_1 = 2.4$, 1.4 and 0.4). The parameters of the coupled system considered are: $m_2/m_1 = 1$, $\xi_1 = \xi_2 = 0.02$, $\omega_1/\omega_2 = 2$ and $\omega/\omega_1 = 0.625$. The figure indicates that there exists three distinct velocity response modes of the connected structures i.e. stick–stick, stick–slip and slip–slip mode for $f_s/a_0m_1 = 2.4$, 1.4 and 0.4, respectively. For relatively higher values of f_s, both structures vibrate together with identical response referred as stick–stick mode (refer Fig. 2(a)). However, with decrease in f_s, the mode of vibration shifts to stick–slip (partial stick and slip motion) or slip–slip mode (complete slip motion in one cycle) from the stick–stick mode as shown in Fig. 2(b) and (c), respectively. Thus, there exist three types of periodic motions namely, stick–stick, stick–slip and slip–slip motions in the harmonic response of structures connected with a friction damper.

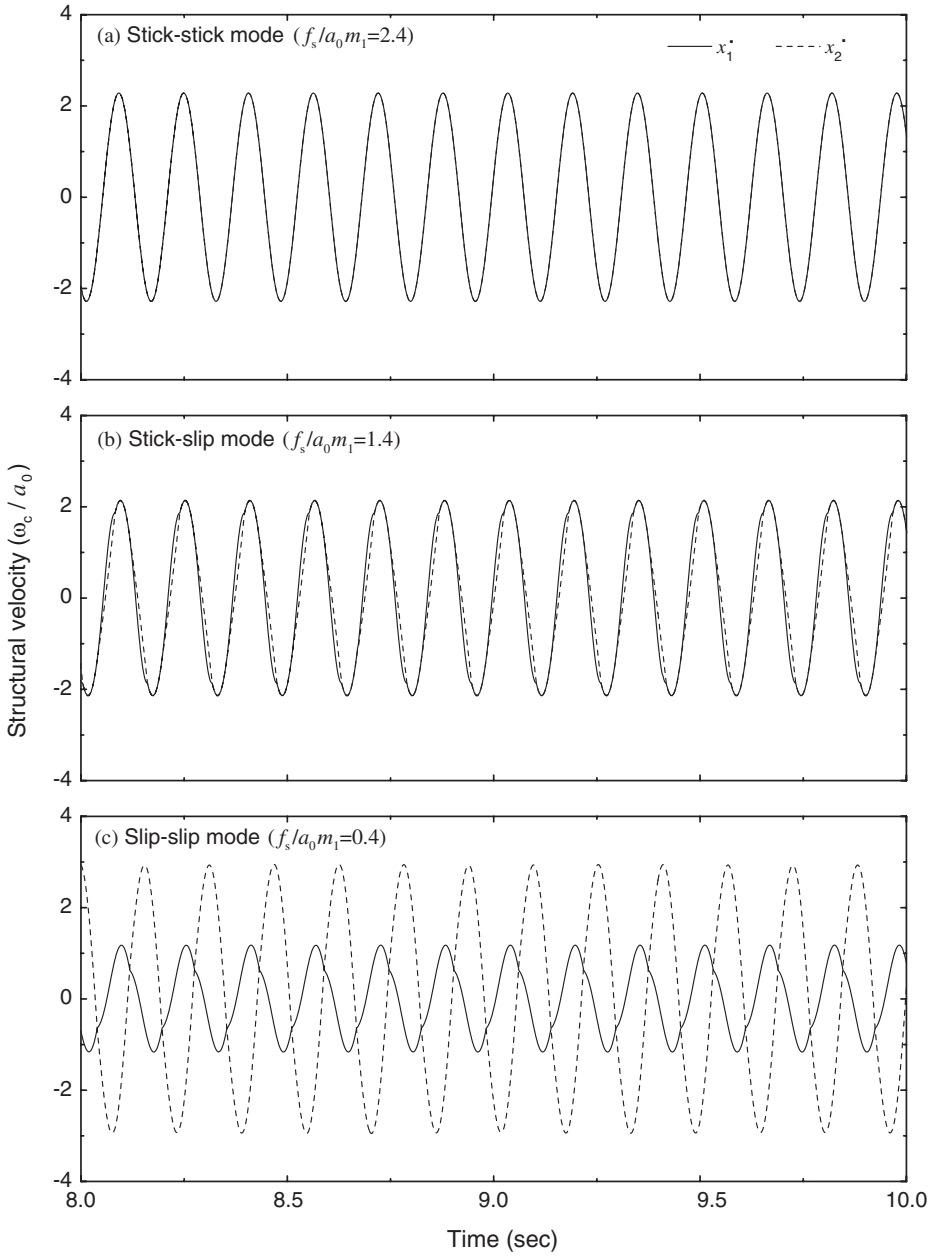

Fig. 2. Velocity responses of the connected structures in the three modes ($m_2/m_1 = 1$, $\xi_1 = \xi_2 = 0.02$, $\omega_1/\omega_2 = 2$ and $\omega/\omega_1 = 0.625$).

3.1. Condition for stick–stick mode

Consider a typical enlarged time history of the velocity response of two structures in the stick–slip mode as shown in Fig. 3. The system is vibrating in slip mode between points A and B, while it is vibrating in stick mode between points B and C. Let t_0 and t_1 denote the time for points B and C, respectively. When point B coincides with point A, the entire mode of vibration becomes stick–stick from the stick–slip mode. Therefore, at the initiation of slippage, we have $t_1 - t_0 = \pi/\omega$. Substituting this relation in Eq. (2), we have

$$\begin{bmatrix} x_c(t_1) \\ \dot{x}_c(t_1) \end{bmatrix} = A_{\mathrm{st}}\left(\frac{\pi}{\omega}\right)\begin{bmatrix} x_c(t_0) \\ \dot{x}_c(t_0) \end{bmatrix} + B_{\mathrm{st}}\left(\frac{\pi}{\omega}\right) = -\begin{bmatrix} x_c(t_0) \\ \dot{x}_c(t_0) \end{bmatrix}. \tag{17}$$

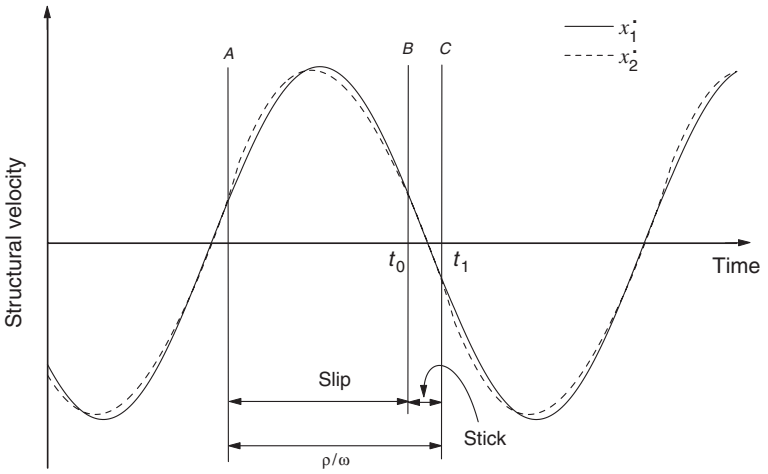

Fig. 3. Typical velocity responses of connected structures in stick–slip mode.

Therefore, $x_c(t_0)$ and $\dot{x}_c(t_0)$ can now be represented as

$$\begin{bmatrix} x_c(t_0) \\ \dot{x}_c(t_0) \end{bmatrix} = -\left[A_{\mathrm{st}}\left(\frac{\pi}{\omega}\right) + I\right]^{-1} B_{\mathrm{st}}\left(\frac{\pi}{\omega}\right), \tag{18}$$

where I is an identity matrix.

Substituting Eqs. (3) and (4) in the above Eq. (18), we get

$$\begin{bmatrix} x_c(t_0) \\ \dot{x}_c(t_0) \end{bmatrix} = \frac{a_0}{\omega_c^2} \begin{bmatrix} b \\ \omega a \end{bmatrix}. \tag{19}$$

Considering Eq. (7a), the condition for stick–stick mode at time $t = t_0$ becomes

$$|m_1 \ddot{x}_c(t_0) + m_1 a_0 \sin(\omega t_0) + c_1 \dot{x}_c(t_0) + k_1 x_c(t_0)| \leqslant f_s. \tag{20}$$

Using Eq. (1), the above equation can be rewritten as

$$|-2\xi_c \omega_c \dot{x}_c(t_0) - \omega_c^2 x_c(t_0) + 2\xi_1 \omega_1 \dot{x}_c(t_0) + \omega_1^2 x_c(t_0)| \leqslant f_s/m_1. \tag{21}$$

Now using Eq. (19), Eq. (21) takes the form given by

$$\left|(2\xi_1 \omega_1 - 2\xi_c \omega_c)\left(\frac{\omega}{\omega_c^2}\, a_0 a\right) + (\omega_1^2 - \omega_c^2)\left(\frac{a_0 b}{\omega_c^2}\right)\right| \leqslant f_s/m_1. \tag{22}$$

Substituting Eqs. (5) and (6) in Eq. (22) and simplifying, we get

$$\left| a_0 \sqrt{\frac{\left(1 - \frac{\omega_1^2}{\omega_c^2}\right)^2 + \left(1 - \frac{\omega_1 \xi_1}{\omega_c \xi_c}\right)^2 \left(2\xi_c \frac{\omega}{\omega_c}\right)^2}{\left(1 - \frac{\omega^2}{\omega_c^2}\right)^2 + \left(2\xi_c \frac{\omega}{\omega_c}\right)^2}} \sin(\omega t_0 - \theta) \right| \leqslant f_s/m_1, \tag{23}$$

$$\tan\theta = \frac{\left(2\xi_c \frac{\omega}{\omega_c}\right)\left[\frac{\omega_1 \xi_1}{\omega_c \xi_c}\left(\frac{\omega_c^2 - \omega^2}{\omega_c^2}\right) - \left(\frac{\omega_1^2 - \omega^2}{\omega_c^2}\right)\right]}{4\xi_c^2 \left(\frac{\omega^2}{\omega_c^2}\right)\left(1 - \frac{\omega_1 \xi_1}{\omega_c \xi_c}\right) + \left(1 - \frac{\omega_1^2}{\omega_c^2}\right)\left(1 - \frac{\omega^2}{\omega_c^2}\right)}. \tag{24}$$

The maximum of absolute value in Eq. (23) should be considered to yield the necessary condition for stick–stick mode expressed by

$$\left| a_0 \sqrt{\frac{\left(1-\frac{\omega_1^2}{\omega_c^2}\right)^2+\left(1-\frac{\omega_1\xi_1}{\omega_c\xi_c}\right)^2\left(2\xi_c\,\frac{\omega}{\omega_c}\right)^2}{\left(1-\frac{\omega^2}{\omega_c^2}\right)^2+\left(2\xi_c\,\frac{\omega}{\omega_c}\right)^2}} \right| \leqslant f_s/m_1. \tag{25}$$

3.2. Condition for initiation of slip–slip mode

The system remains in slip–slip mode when point B coincides with point C as shown in Fig. 3. Let the slippage starts at time t_0^* and continues till time t_1^*, we have $t_1^* - t_0^* = \pi/\omega$. Substituting this into Eq. (11) and considering the periodicity of the solution yields to

$$\begin{bmatrix} x_1(t_1^*) \\ \dot{x}_1(t_1^*) \end{bmatrix} = A_{\mathrm{sl}}\left(\frac{\pi}{\omega}\right)\begin{bmatrix} x_1(t_0^*) \\ \dot{x}_1(t_0^*) \end{bmatrix} + B_{\mathrm{sl}}\left(\frac{\pi}{\omega}\right) = -\begin{bmatrix} x_1(t_0^*) \\ \dot{x}_1(t_0^*) \end{bmatrix}. \tag{26}$$

Therefore, the displacement and the velocity at time $t = t_0^*$ can be expressed by

$$\begin{bmatrix} x_1(t_0^*) \\ \dot{x}_1(t_0^*) \end{bmatrix} = -\left[A_{\mathrm{sl}}\left(\frac{\pi}{\omega}\right) + I\right]^{-1} B_{\mathrm{sl}}\left(\frac{\pi}{\omega}\right). \tag{27}$$

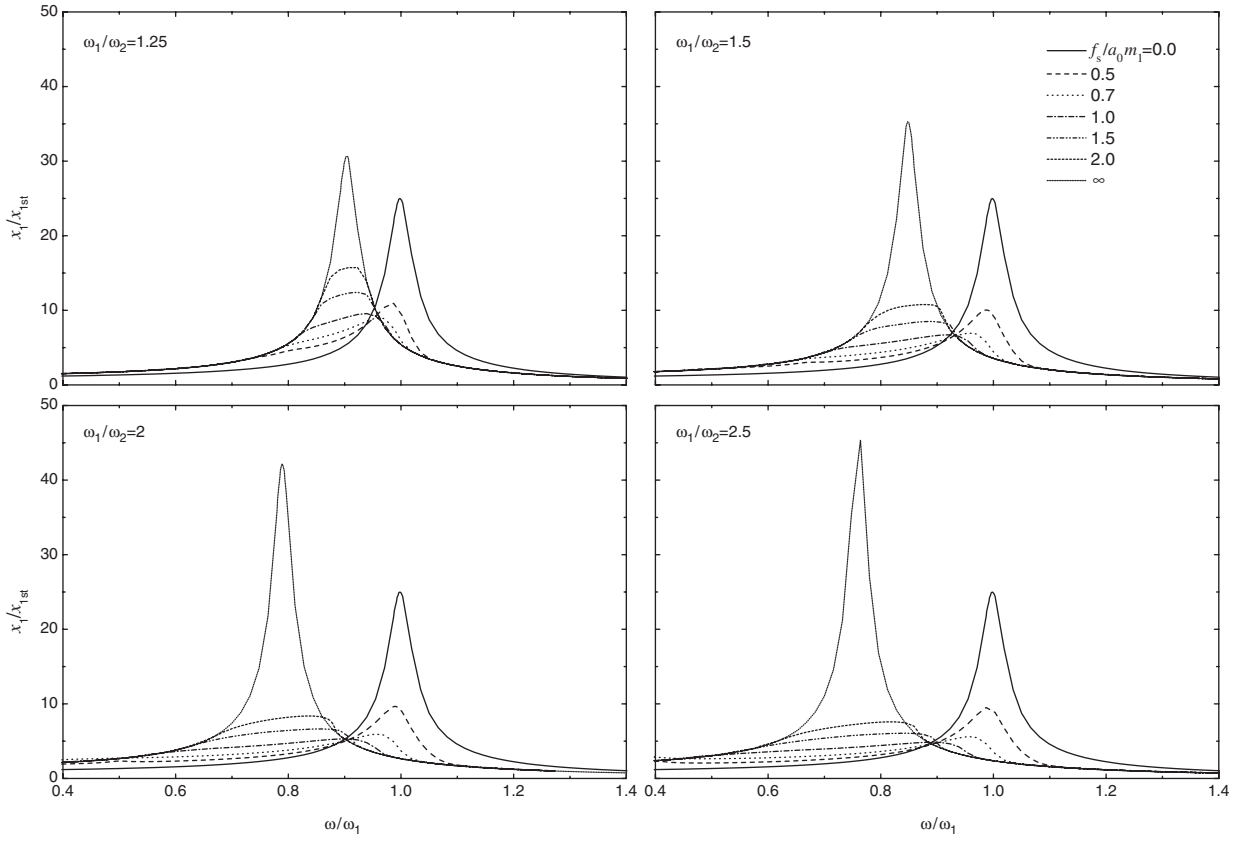

Fig. 4. Variation of peak displacement response ratio of Structure-1 with excitation frequency ratio ($m_2/m_1 = 1$ and $\xi_1 = \xi_2 = 0.02$).

Substituting Eqs. (12) and (13) in Eq. (27) and simplifying, it leads to

$$x_1(t_0^*) = \frac{a_0}{\omega_1^2}\, b' + \frac{\frac{\xi_1}{\sqrt{1-\xi_1^2}} \sin\left(\pi \frac{\omega_1'}{\omega}\right) - \sinh\left(\pi\xi_1 \frac{\omega_1}{\omega}\right)}{\cos\left(\pi \frac{\omega_1'}{\omega}\right) + \cosh\left(\pi\xi_1 \frac{\omega_1}{\omega}\right)} f_s/k_1, \tag{28}$$

$$\dot{x}_1(t_0^*) = \frac{a_0}{\omega_1^2}\, \omega a' - \frac{\frac{\omega_1}{\sqrt{1-\xi_1^2}} \sin\left(\pi \frac{\omega_1'}{\omega}\right)}{\cos\left(\pi \frac{\omega_1'}{\omega}\right) + \cosh\left(\pi\xi_1 \frac{\omega_1}{\omega}\right)} f_s/k_1. \tag{29}$$

Considering Eq. (8a), the expression for slip–slip mode at time $t = t_0^*$ becomes

$$|m_1\ddot{x}_1(t_0^*) + m_1 a_0 \sin(\omega t_0^*) + c_1\dot{x}_1(t_0^*) + k_1 x_1(t_0^*)| > f_s. \tag{30}$$

Using Eq. (1) and noting that at the initiation of slippage $x_1 = x_c$, the above equation can be rewritten as

$$|-2\xi_c\omega_c\dot{x}_1(t_0^*) - \omega_c^2 x_1(t_0^*) + 2\xi_1\omega_1\dot{x}_1(t_0^*) + \omega_1^2 x_1(t_0^*)| > f_s/m_1. \tag{31}$$

Substituting for displacement and velocity using Eqs. (28) and (29) in Eq. (31) and simplifying using Eqs. (14) and (15), it takes the form given by

$$|a_0\alpha \sin(\omega t_0^* - \theta_0) + \beta| > f_s/m_1, \tag{32}$$

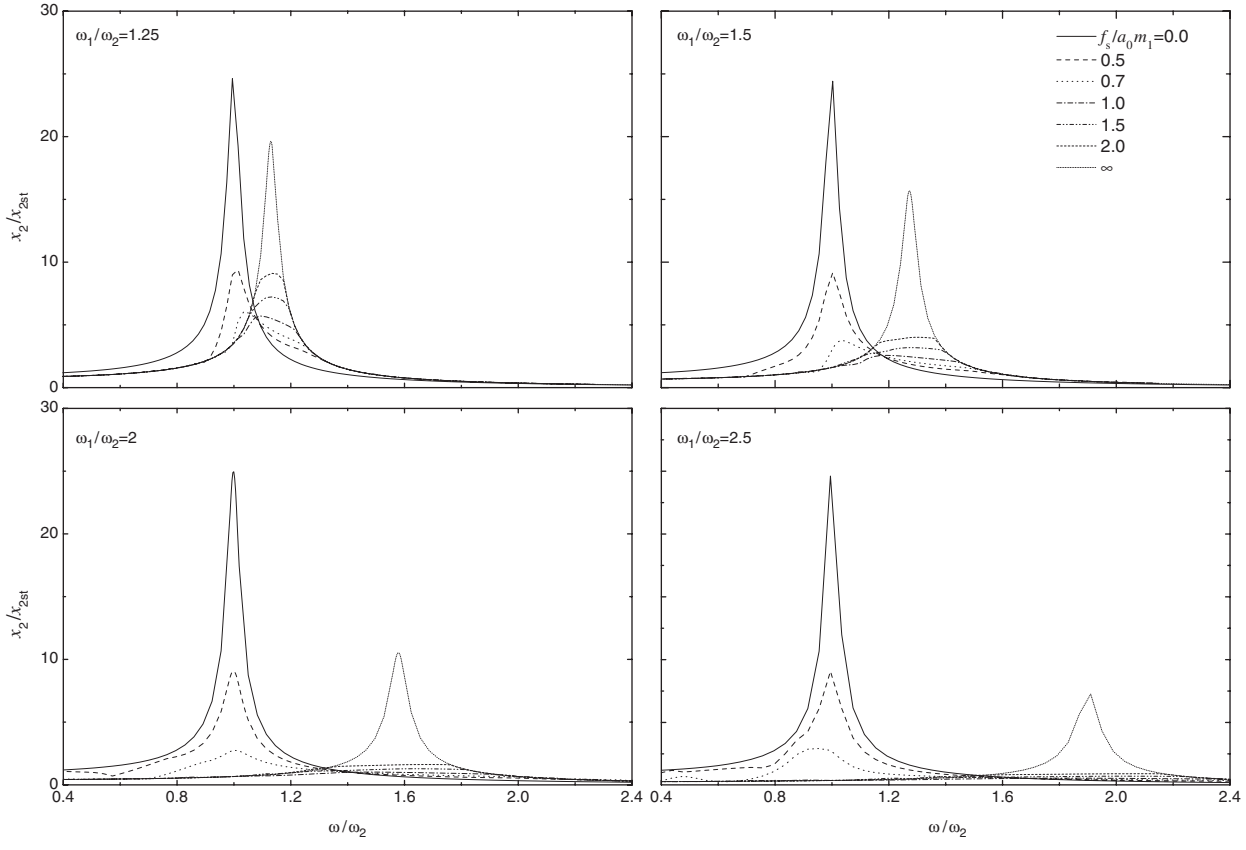

Fig. 5. Variation of peak displacement response ratio of Structure-2 with excitation frequency ratio ($m_2/m_1 = 1$ and $\xi_1 = \xi_2 = 0.02$).

where

$$\alpha = \sqrt{\frac{\left(1-\frac{\omega_c^2}{\omega_1^2}\right)^2 + \left(1-\frac{\omega_c\xi_c}{\omega_1\xi_1}\right)^2\left(2\xi_1\,\frac{\omega}{\omega_1}\right)^2}{\left(1-\frac{\omega^2}{\omega_1^2}\right)^2 + \left(2\xi_1\,\frac{\omega}{\omega_1}\right)^2}}, \tag{33}$$

$$\tan\,\theta_0 = \frac{\left(2\xi_1\,\frac{\omega}{\omega_1}\right)\left(\frac{\omega_c\xi_c}{\omega_1\xi_1}-\frac{\omega_c^2}{\omega_1^2}\right) + \left(1-\frac{\omega_c\xi_c}{\omega_1\xi_1}\right)2\xi_1\left(\frac{\omega}{\omega_1}\right)^3}{\left[\left(1-\frac{\omega_c\xi_c}{\omega_1\xi_1}\right)4\xi_1^2 - \left(1-\frac{\omega_c^2}{\omega_1^2}\right)\right]\left(\frac{\omega}{\omega_1}\right)^2 + \left(1-\frac{\omega_c^2}{\omega_1^2}\right)}, \tag{34}$$

$$\beta = \frac{(\omega_1^2-\omega_c^2)\sinh\,\phi - c_n\,\sin\,\psi}{\cosh\,\phi + \cos\,\psi}\,(f_s/k_1)\mathrm{sgn}(\dot{x}_2-\dot{x}_1), \tag{35}$$

$$c_n = \frac{1}{\sqrt{1-\xi_1^2}}(2\omega_1\omega_c\xi_c - \xi_1\omega_c^2 - \xi_1\omega_1^2), \tag{36}$$

$$\phi = \pi\xi_1\,\frac{\omega_1}{\omega}, \tag{37}$$

$$\psi = \pi\,\frac{\omega_1'}{\omega}. \tag{38}$$

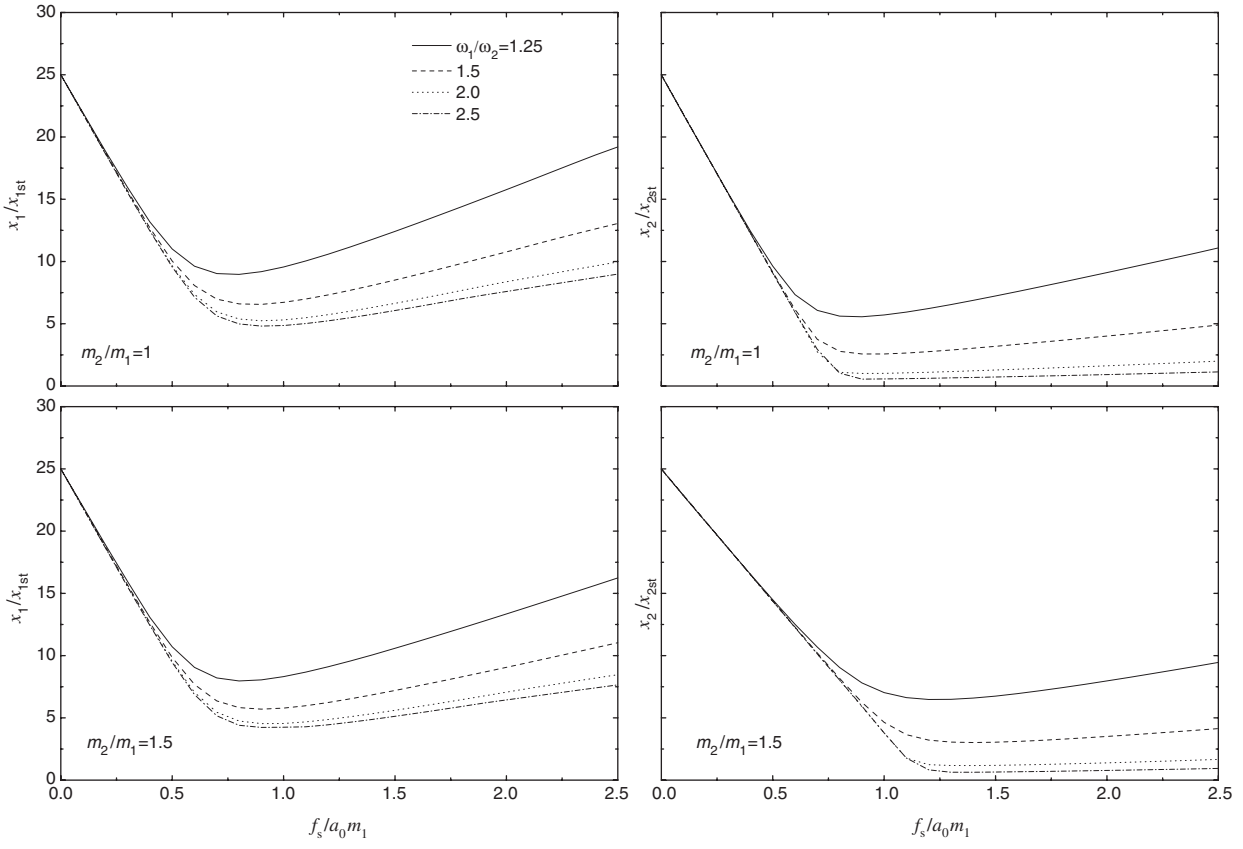

Fig. 6. Variation of peak displacement response ratios with damper slip force ($m_2/m_1 = 1$ and $\xi_1 = \xi_2 = 0.02$).

The maximum of absolute value in Eq. (32) yields the condition for the system to be in slip–slip mode given by

$$|a_0\alpha + \beta| > f_s/m_1. \tag{39}$$

3.3. Conditions for three periodic modes

The conditions for three periodic modes to occur in the harmonic response of adjacent structures connected with a friction damper are expressed as follows:

(a) Stick–stick mode:

$$\left| a_0 \sqrt{\frac{\left(1-\frac{\omega_1^2}{\omega_c^2}\right)^2 + \left(1-\frac{\omega_1\xi_1}{\omega_c\xi_c}\right)^2\left(2\xi_c\,\frac{\omega}{\omega_c}\right)^2}{\left(1-\frac{\omega^2}{\omega_c^2}\right)^2 + \left(2\xi_c\,\frac{\omega}{\omega_c}\right)^2}} \right| \leqslant f_s/m_1. \tag{40}$$

(b) Stick–slip mode:

$$|a_0\alpha + \beta| \leqslant f_s/m_1 < \left| a_0 \sqrt{\frac{\left(1-\frac{\omega_1^2}{\omega_c^2}\right)^2 + \left(1-\frac{\omega_1\xi_1}{\omega_c\xi_c}\right)^2\left(2\xi_c\,\frac{\omega}{\omega_c}\right)^2}{\left(1-\frac{\omega^2}{\omega_c^2}\right)^2 + \left(2\xi_c\,\frac{\omega}{\omega_c}\right)^2}} \right|. \tag{41}$$

Table 1
Optimum damper slip force and percentage of reductions in the peak displacement responses of coupled structures

Response	m_2/m_1	ξ_1	ξ_2	Optimum f_s (a_0m_1)				Percentage response reduction			
				$\omega_1/\omega_2 = 1.25$	1.5	2.0	2.5	$\omega_1/\omega_2 = 1.25$	1.5	2.0	2.5
x_1	1	0.02	0.02	0.769	0.878	0.908	0.920	64.21	73.92	79.10	80.76
		0.02	0.05	0.799	0.870	0.904	0.931	64.06	73.67	78.93	80.64
		0.05	0.02	0.501	0.629	0.697	0.740	36.25	49.39	57.44	60.23
		0.05	0.05	0.501	0.622	0.689	0.739	36.01	48.71	57.09	59.96
	1.5	0.02	0.02	0.809	0.939	0.932	0.925	68.29	77.21	81.94	83.38
		0.02	0.05	0.781	0.903	0.927	0.960	67.89	76.89	81.75	83.30
		0.05	0.02	0.539	0.697	0.740	0.787	40.50	53.88	61.83	64.49
		0.05	0.05	0.512	0.690	0.738	0.779	39.17	53.11	61.25	64.16
	2	0.02	0.02	0.800	0.911	0.968	0.813	70.22	79.04	83.42	83.76
		0.02	0.05	0.848	0.898	0.962	0.838	69.74	78.67	83.23	84.06
		0.05	0.02	0.589	0.698	0.789	0.762	41.34	56.52	64.27	66.73
		0.05	0.05	0.590	0.689	0.779	0.753	41.24	55.67	63.78	66.41
x_2	1	0.02	0.02	0.873	0.972	0.930	0.891	77.78	89.78	95.96	97.77
		0.02	0.05	0.640	0.842	0.872	0.860	56.10	77.32	90.45	94.65
		0.05	0.02	0.898	0.959	0.923	0.886	77.93	89.67	95.90	97.75
		0.05	0.05	0.672	0.832	0.866	0.848	56.08	77.02	90.29	94.54
	1.5	0.02	0.02	1.271	1.361	1.378	1.344	74.26	87.94	95.33	97.75
		0.02	0.05	0.923	1.160	1.270	1.290	51.30	73.92	89.05	93.92
		0.05	0.02	1.251	1.390	1.350	1.350	74.56	87.87	94.90	97.40
		0.05	0.05	0.905	1.190	1.259	1.297	51.28	73.73	89.02	93.76
	2	0.02	0.02	1.487	1.895	1.805	1.820	70.96	86.19	94.74	97.04
		0.02	0.05	1.047	1.569	1.661	1.739	47.19	70.85	87.80	92.94
		0.05	0.02	1.510	1.881	1.779	1.848	71.21	86.18	94.63	96.94
		0.05	0.05	1.052	1.560	1.641	1.769	47.14	70.71	87.53	92.72

(c) Slip–slip mode:

$$|a_0\alpha + \beta| > f_s/m_1. \tag{42}$$

4. Parametric study

In this section, a detailed parametric study is conducted to investigate the influence of system parameters on the harmonic response of structures connected with friction damper. The important parameters considered are frequency ratio (ω_1/ω_2), mass ratio (m_2/m_1), damping ratios of the two structures (ξ_1 and ξ_2), slip force (f_s), and excitation frequency (ω). The above structural parameters are varied by changing the properties of Structure-2 but keeping the same properties of Structure-1. The response quantities of interest are the displacement of adjacent structures (i.e. x_1 and x_2) relative to the ground and the displacement in the friction damper. The relative displacement of structures is important, as the stresses in the structural members are directly proportional to it. On the other hand, the displacement in friction damper is crucial from design point of view. In addition, the optimum value of slip force in the friction damper for minimum displacement response of connected structures is also investigated. The results of the parametric study are presented in non-dimensional form. The displacement responses of the two structures are normalized with their corresponding static displacements i.e. x_{1st} and x_{2st}. The maximum displacement in the damper is expressed as a dimensionless parameter by multiplying with either ω_c^2/a_0 or ω_1^2/a_0.

In order to study the effects of slip force, the variation of peak relative displacement of the Structure-1 (stiffer) is plotted in Fig. 4 against the excitation frequency for various values of f_s (i.e. varying from zero to infinity). The zero value of f_s implies that the two structures are without friction damper. On the other hand,

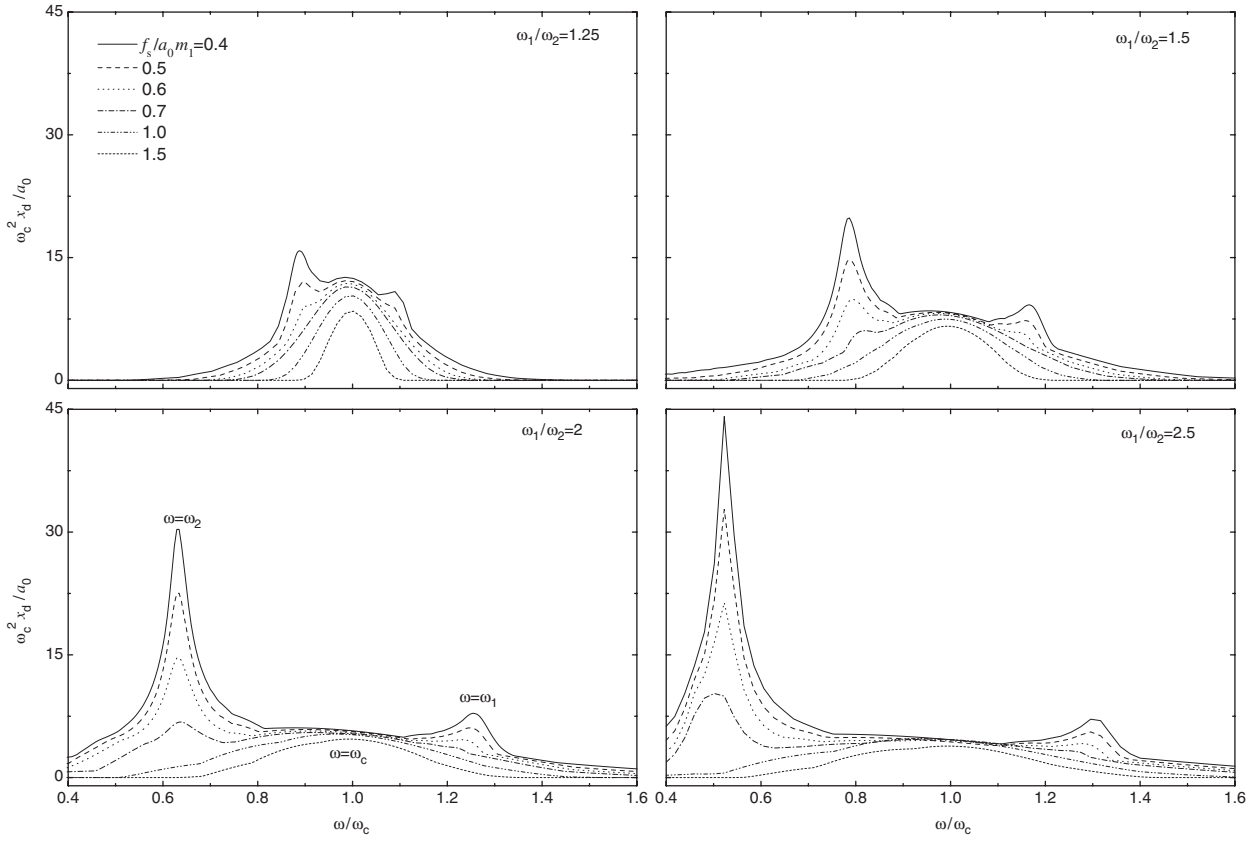

Fig. 7. Effects of slip force on maximum displacement in the damper ($m_2/m_1 = 1$ and $\xi_1 = \xi_2 = 0.02$).

infinite value of f_s implies that the two structures are connected with a rigid link. It is observed from Fig. 4 that the peak displacement of the Structure-1 reduces up to a certain increase in the value of f_s for all values of ω_1/ω_2 ratios. However, with further increase in the f_s, the peak displacement of the structure increases. For higher values of the f_s, the peak response of the structure becomes more than that without any damper (compare the response for f_s equal to 0 and ∞). This shows that there exists an optimum value of slip force for which the peak displacement of the structure attains the minimum value. At optimum value of the slip force, there is significant reduction in the peak response of the structure implying that the friction damper is very effective in controlling the dynamic response of connected structures. The similar effects of slip force of the damper are depicted in Fig. 5 showing the corresponding peak harmonic displacement of Structure-2.

The variations of the peak displacements of two structures are shown in Fig. 6 against damper slip force for different values of mass ratios (i.e. $m_2/m_1 = 1$ and 1.5) and frequency ratios ($\omega_1/\omega_2 = 1.25$, 1.5, 2 and 2.5). As observed earlier, there exists an optimum value of damper slip force for minimum displacement of connected structures. The optimum slip force marginally increases with the increase of frequency ratio, ω_1/ω_2 for both structures. The peak displacement of the structures decreases with the increase of the frequency ratio, ω_1/ω_2. This implies that the friction damper performs better when frequencies of the connected structures are well separated. This is expected due to the fact that when frequencies are well separated, the adjacent structures vibrate out of phase causing large displacements in the damper thereby dissipation of large input energy through friction and subsequent reduction in the dynamic response of the system.

In Table 1, the optimum slip force and corresponding displacement reduction of two adjacent structures are shown for different combinations of parameters ξ_1, ξ_2, ω_1/ω_2 and m_2/m_1. The various observations made from the Table 1 are: (i) the optimum slip force is different for each of the two connected structures, (ii) the optimum slip force and corresponding reduction in the response for a structure depends on its own damping

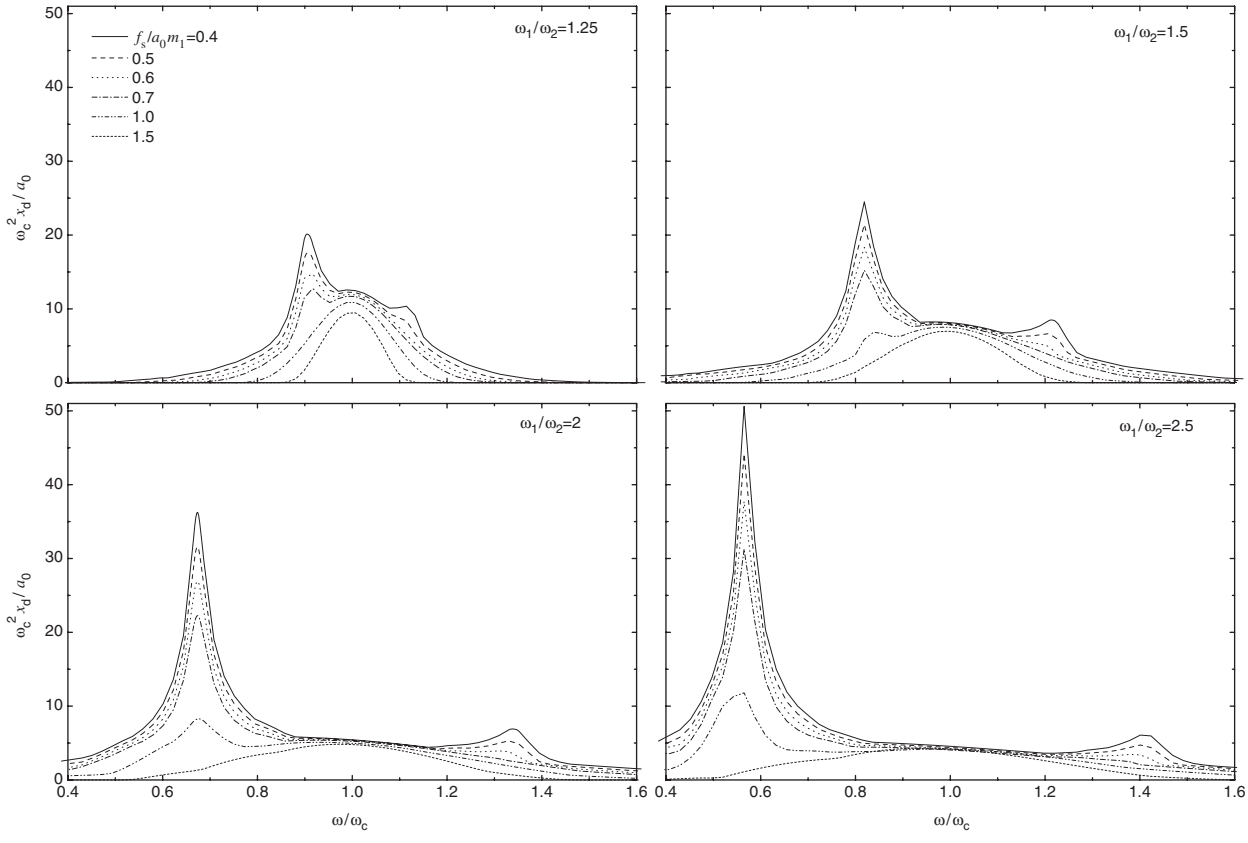

Fig. 8. Effects of slip force on maximum displacement in the damper ($m_2/m_1 = 1.5$ and $\xi_1 = \xi_2 = 0.02$).

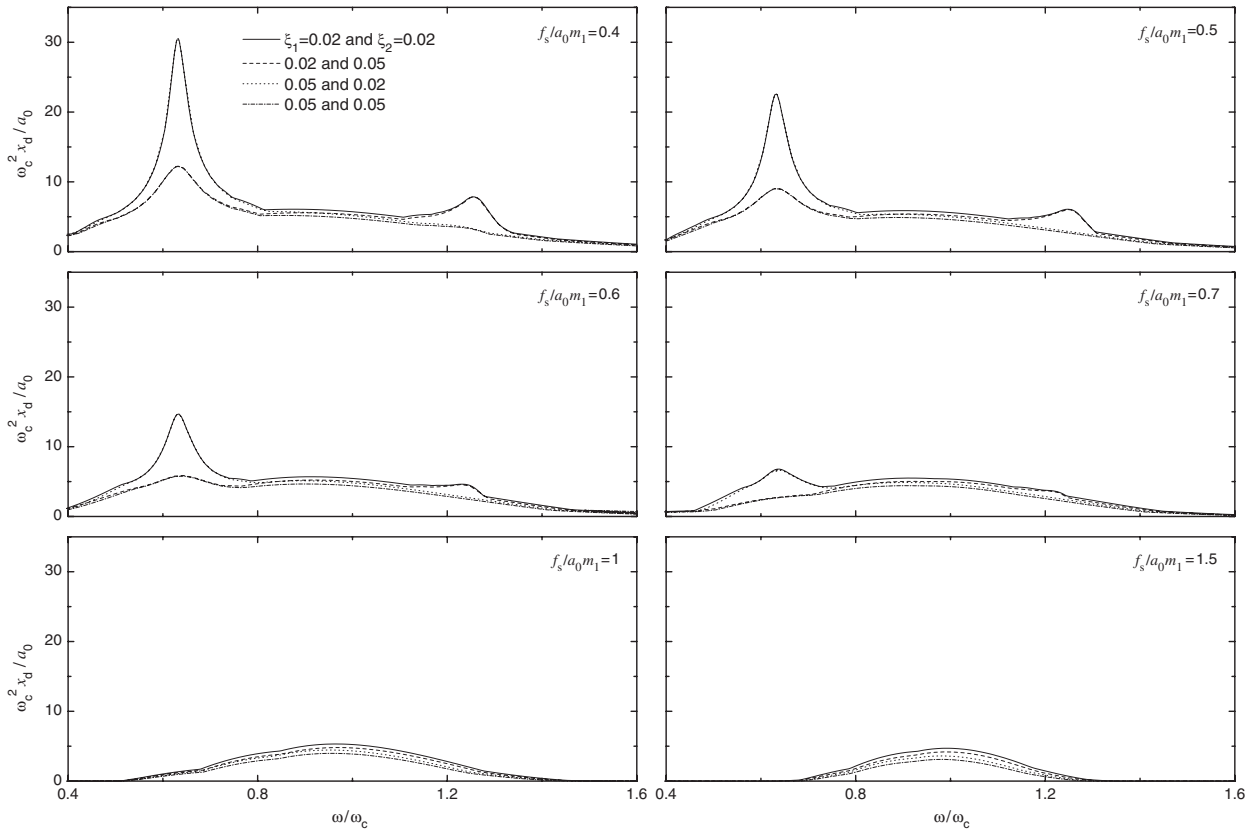

Fig. 9. Effects of damping ratios on maximum displacement in the damper ($m_2/m_1 = 1$ and $\omega_1/\omega_2 = 2$).

ratio rather than the damping ratio of adjacent structure, (iii) the optimum slip force increases marginally with the increase of frequency ratio, (iv) the optimum slip force of a structure increases with the increase of its mass provided the other parameters held constant and (v) the reduction in response increases with the increase of frequency ratio and it is higher for softer structure as compared to stiffer structure.

The effects of slip force on the absolute maximum displacement in the damper, $x_d = |(x_2 - x_1)|_{\max}$ is shown in Figs. 7 and 8 for $m_2/m_1 = 1$ and 1.5, respectively. The results are shown for various frequency ratios and considering damping ratio in both structures as 0.02. It is observed that as the slip force increases (i.e. the damper becomes more stiff) the damper displacement decreases. The maximum value of damper displacement occurs when excitation frequency is in the vicinity of three natural frequencies (i.e. ω_1, ω_2 and ω_c) depending upon the magnitude of the slip force. For low values of slip force, the peak damper displacement occurs when the system is excited to the frequency of the softer building (ω_2). However, for higher values of the slip force the maximum damper displacement occur in the vicinity of combined frequency (ω_c). The peak displacement of damper with low slip force increases with increase of frequency ratio. On the other hand, opposite trend is observed for damper with higher slip force.

The effect of damping ratios of coupled structures on the damper displacement is shown in Fig. 9 by considering four sets of structure damping ratios. It is seen from Fig. 9 that the maximum damper displacement reduces significantly with the increase of the damping of softer structure. The damper displacement is not much sensitive to level of damping in stiffer structure in the range of parameters for practical applications. Thus, the damping of softer structure has significant influence on the maximum displacement in damper. The effect of mass ratio on the damper displacement is shown in Fig. 10. It is observed that the damper displacement increases with increase of the mass ratio. This may be due to the reason that higher mass ratio changes the dynamic characteristics and response of two connected structure which causes higher damper displacement.

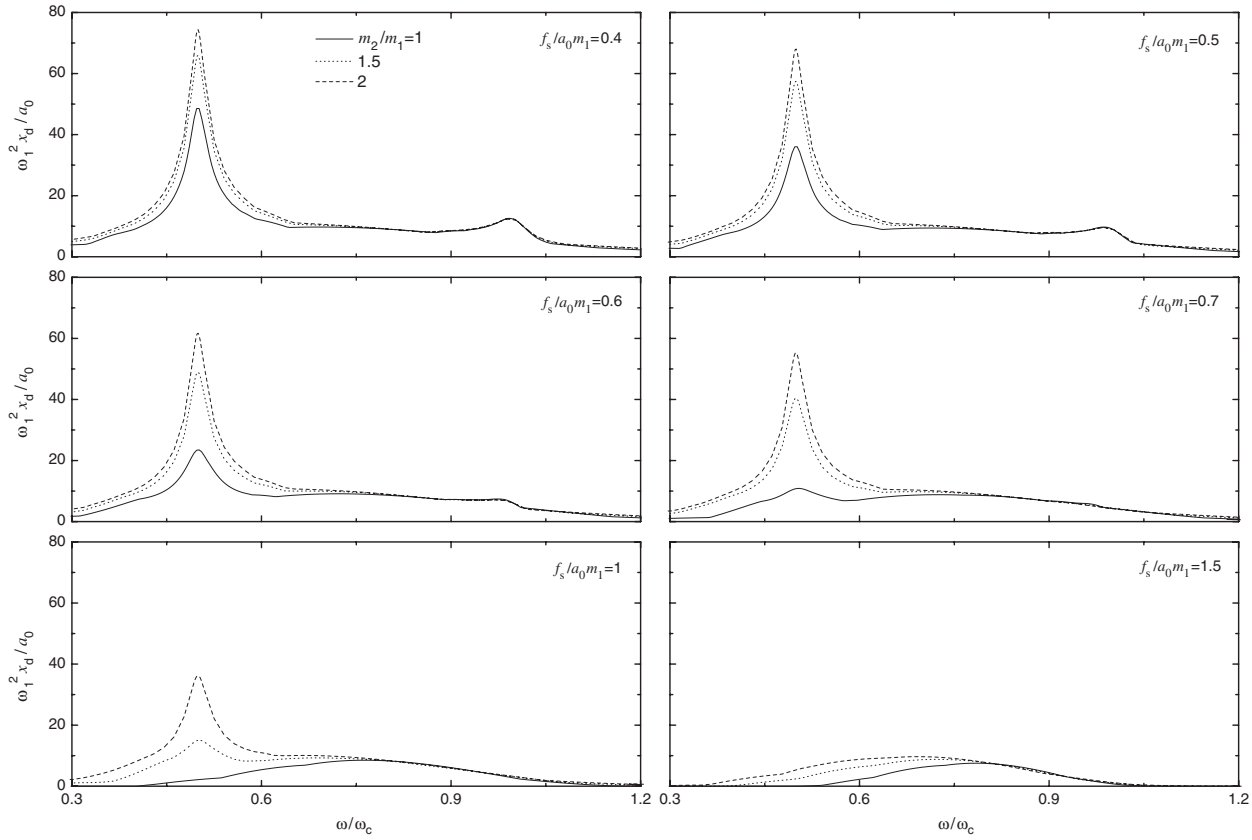

Fig. 10. Effects of mass ratio on maximum displacement in the damper ($\xi_1 = \xi_2 = 0.02$, and $\omega_1/\omega_2 = 2$).

5. Conclusions

The dynamic behavior of two adjacent structures connected with friction damper is investigated under harmonic ground excitation. The governing equations of motion of the coupled system are derived and solved for finding out responses during non-slip and slip phases of friction damper. The explicit expressions for conditions of various modes of the periodic response of connected structures are derived. From the trends of the results of the present study, the following conclusions may be drawn:

1. There exist three types of periodic motion, namely stick–stick, stick–slip and slip–slip motions in the harmonic response of adjacent structures connected with friction damper.
2. The friction damper is found to be effective in reducing the dynamic response of connected structures. The friction dampers are more effective when the natural frequencies of the connected structures are well separated.
3. The friction damper is found to be more beneficial for softer structure in comparison to the stiff structure of the combined system.
4. There exists an optimum slip force in the damper for which the peak displacement of a structure attains the minimum value. The optimum slip force is different for each of the two connected structures.
5. The optimum slip force and percentage reduction in the displacement of a structure depend on its own damping ratio rather than damping in the adjacent structure.
6. The maximum displacement in friction damper reduces as the slip force increases and it also increases with the increase in the mass ratio of the connected structures. The damper displacement significantly decreases with increase of damping in the softer structure.

References

[1] G.W. Housner, L.A. Bergman, T.K. Caughey, A.G. Chassiakos, R.O. Claus, S.F. Masri, R.E. Skelton, T.T. Soong, B.F. Spencer, J.T.P. Yao, Structural control: past, present, and future, *Journal of Engineering Mechanics, ASCE* 123 (1997) 897–971.

[2] B. Westermo, The dynamics of inter-structural connection to prevent pounding, *Earthquake Engineering and Structural Dynamics* 18 (1989) 687–699.

[3] J.E. Luco, F.C.P. De Barros, Optimal damping between two adjacent elastic structures, *Earthquake Engineering and Structural Dynamics* 27 (1998) 649–659.

[4] W.S. Zhang, Y.L. Xu, Vibration analysis of two buildings linked by Maxwell Model-defined fluid dampers, *Journal of Sound and Vibration* 233 (2000) 775–796.

[5] H.P. Zhu, H. Iemura, A study of response control on the passive coupling element between two parallel structures, *Structural Engineering and Mechanics* 9 (2000) 383–396.

[6] Y.Q. Ni, J.M. Ko, Z.G. Ying, Random seismic response analysis of adjacent buildings coupled with non-linear hysteretic dampers, *Journal of Sound and Vibration* 246 (2001) 403–417.

[7] A.S. Pall, C. Marsh, Response of friction damped braced frames, *Journal of Structural Division, ASCE* 108 (1982) 1313–1323.

[8] W.L. Qu, Z.H. Chen, Y.L. Xu, Dynamic analysis of wind-excited truss tower with friction dampers, *Computers and Structures* 79 (2001) 2817–2831.

[9] I.H. Mualla, B. Belev, Performance of steel frames with a new friction damper device under earthquake excitation, *Engineering Structures* 24 (2002) 365–371.

[10] C. Pasquin, N. Leboeuf, R.T. Pall, A.S. Pall, Friction dampers for seismic rehabilitation of Eaton's building, Montreal, *Thirteenth World Conference on Earthquake Engineering*, Paper No. 1949, 2004.

[11] B. Westermo, F. Udwadia, Periodic response of sliding oscillator system to harmonic excitation, *Earthquake Engineering and Structural Dynamics* 11 (1982) 135–146.

[12] C.J. Younis, I.G. Tadjbakhsh, Response of sliding rigid structure to base excitation, *Journal of Engineering Mechanics, ASCE* 110 (1984) 417–432.

[13] K. Matsui, M. Iura, T. Sasaki, I. Kosaka, Periodic response of a rigid block resting on a footing subjected to harmonic excitation, *Earthquake Engineering and Structural Dynamics* 20 (1991) 683–697.

[14] M. Iura, K. Matsui, I. Kosaka, Analytical expressions for three different modes in harmonic motion of sliding structures, *Earthquake Engineering and Structural Dynamics* 21 (1992) 757–769.